

The effect of Zn-Sn pair-doping on M-type Sr-hexaferrite

Laalitha S. I. Liyanage

*Department of Physics and Astronomy, Mississippi State University, Mississippi State, MS 39762, USA and
Center for Advanced Vehicular Systems, Mississippi State University, Mississippi State, MS 39762, USA*

Sungho Kim

Center for Computational Sciences, Mississippi State University, Mississippi State, MS 39762, USA

Yang Ki Hong and Ji-Hoon Park

*Department of Electrical and Computer Engineering and MINT Center,
The University of Alabama, Tuscaloosa, AL 35487*

Steven C. Erwin

Center for Computational Materials Science, Naval Research Laboratory, Washington, D.C. 20375, USA

Seong-Gon Kim*

*Department of Physics and Astronomy, Mississippi State University, Mississippi State, MS 39762, USA and
Center for Computational Sciences, Mississippi State University, Mississippi State, MS 39762, USA
(Dated: September 25, 2012)*

We study the site occupancy and magnetic properties of Zn-Sn substituted M-type Sr-hexaferrite $\text{SrFe}_{12-x}(\text{Zn}_{0.5}\text{Sn}_{0.5})_x\text{O}_{19}$ with $x = 1$ using first-principles total-energy calculations. We find that in a ground-state configuration Zn-Sn ions preferentially occupy $4f_1$ and $4f_2$ sites unlike the model previously suggested by Ghasemi et al. [J. Appl. Phys, **107**, 09A734 (2010)], where Zn-Sn ions occupy $2b$ and $4f_2$ sites. Our model predicts a rapid increase in saturation magnetic moment (M_s) as well as decrease in magnetic anisotropy compared to the pure M-type Sr-hexaferrite consistent with experimental observations.

I. INTRODUCTION

Strontium hexaferrite $\text{SrFe}_{12}\text{O}_{19}$ (SrM) is widely used as a material for permanent magnets along with other M-type hexaferrites $M\text{Fe}_{12}\text{O}_{19}$ ($M = \text{Sr}, \text{Ba}, \text{Pb}$) due to their high Curie temperatures, large saturation magnetizations (M_s), high value of coercivity, excellent chemical stability and low cost. Recently SrM is investigated for the use in magnetic recording media,¹⁻³ but due to its high intrinsic coercivity, pure SrM is difficult to be used as magnetic recording materials.⁴ Magnetism in SrM results from Fe^{3+} ions occupying five different interstitial sites in the ten oxygen layers of the crystallographic unit cell: three octahedral sites ($12k$, $4f_2$, $2a$), one tetrahedral site ($4f_1$) and one trigonal bipyramid site ($2b$). Investigations to improve the magnetic properties of M-type hexaferrites have been done through substitution of various impurities.¹⁻¹⁹ Substitution of Fe^{3+} ions with transition metal ions have proven to be successful in improving the magnetic properties of SrM. Pair-doping of Fe atoms by Zn-Nb¹⁸, Zr-Cd¹¹, Zn-Sn⁷, Sn-Mg², and Er-Ni³ improved magnetic properties of SrM. Zr-Cd substituted SrM ($\text{SrFe}_{12-x}(\text{Zr}_{0.5}\text{Cd}_{0.5})_x\text{O}_{19}$) showed increase of M_s only up to $x = 0.2$. Coercivity decreased continuously with increase of Zr-Cd concentration¹¹ while M_s and coercivity steadily increased in Er-Ni substituted SrM with Er-Ni concentration. Substitution by Zn-Nb¹⁸, Zn-Sn^{7,20} and Sn-Mg² increased the saturation magnetization (M_s) and decreased coercivity.

Using the density functional theory (DFT) Fang et

al.²¹ investigated the electronic structure of SrM. Novak et al. calculated the electronic structure and exchange interactions of barium hexaferrite using DFT.²² In spite of the importance of substituted SrM, only a few theoretical investigations have been done on La substitution.^{23,24} To our knowledge, no electronic structure calculation has been done on experimental investigations of pair-doped SrM. The knowledge of site occupancy of the substituted atoms and the change in atomic magnetic moments in substituted SrM would be advantageous in understanding the effect of pair-doping on magnetic properties of SrM.

In this work we use first-principles total-energy calculations to study the site preference and magnetic properties of Zn-Sn substituted M-type Sr-hexaferrite $\text{SrFe}_{12-x}(\text{Zn}_{0.5}\text{Sn}_{0.5})_x\text{O}_{19}$ with $x = 1$. Based on total energy calculations, we conclude that in the ground-state configuration Zn-Sn ions preferentially occupy $4f_1$ and $4f_2$ sites in contrast to the model suggested by Ghasemi and co-workers^{7,20}, where Zn-Sn ions occupy $2b$ and $4f_2$ sites. We further show that our model predicts increase in saturation magnetization (M_s) as well as decrease in magnetic anisotropy energy (MAE) compared to the pure M-type Sr-hexaferrite ($x = 0$) consistent with experimental observations.

II. METHODOLOGY

To determine the site preference of Zn and Sn atoms in Sr-hexaferrite, we use first-principles total-energy calculations for configurations of $\text{SrFe}_{12-x}(\text{Zn}_{0.5}\text{Sn}_{0.5})_x\text{O}_{19}$ at $x = 0$ and $x = 1$. $x = 0$ configuration corresponds to the pure SrM without any substitution. We used a unit cell which contains two formula units of SrM in our calculations. $x = 1$ configuration was constructed by substituting Zn and Sn, one atom each, into the Fe sublattices of SrM. Total energies and forces were calculated using density-functional theory (DFT) combined with projector-augmented-wave (PAW) potentials as implemented in VASP.^{25,26} All calculations were spin polarized according to Gorter's ferrimagnetic ordering of Fe spins.²⁷ Brillouin zone sampling was performed using the Monkhorst-Pack scheme²⁸ with a Fermi-level smearing of 0.2 eV applied through the Methfessel-Paxton method²⁹ for relaxations and the tetrahedron method³⁰ for static calculations. Using the quasi-Newton algorithm,³¹ we performed geometric optimizations to relax the positions of ions. Electron exchange and correlation were treated with generalized gradient approximation (GGA) as parameterized by the Perdew-Burke-Ernzerhof (PBE) scheme.³² To improve the description of Fe 3d electrons hybrid functionals in the Heyd-Scuseria-Ernzerhof (HSE) scheme³³⁻³⁵ and GGA+U method were employed. Formula by Vosko et al.³⁶ was used for the interpolation of the correlation part of the electron exchange and correlation potential. A plane-wave energy cutoff of 520 eV was used, and volumetric optimizations were performed to obtain ground state of $\text{SrFe}_{12}\text{O}_{19}$. For $\text{SrFe}_{12-x}(\text{Zn}_{0.5}\text{Sn}_{0.5})_x\text{O}_{19}$, with $x = 1$, only atomic relaxations were performed with a plane-wave energy cutoff of 400 eV. In each case, geometric optimizations were performed until the energy difference between two successive ionic optimization steps was less than 0.001 meV.

A. GGA+U

Although GGA is adequate for most calculations, when applied to systems such as transition metal oxides that contain 3d electrons, it underestimates the band gap and the magnetic moment. Therefore to improve the description of the Fe 3d electrons, we used the simplified rotationally invariant approach to the L(S)DA+U method described by Dudarev et al.,³⁷ with GGA instead of the L(S)DA exchange and correlation functional. The method requires an effective U value (U_{eff}) equal to the difference between the Hubbard parameter U and the exchange parameter J , which is part of the added penalty functional that represents the double counting correction to the total energy of L(S)DA (in our case GGA). The U and J parameters can either be determined from experiments or estimated using restricted L(S)DA (GGA) calculations. Novak et al. performed GGA+U calculations using full potential linearized augmented plane

wave (FPLAPW) method.²² Their calculations compared two values, $U = 3.4$ eV and $U = 6.9$ eV, with GGA which corresponds to $U = 0$ eV. We used the magnetic moment of Fe atoms predicted by calculations using hybrid density functionals to determine the U value. Using the determined U , the electronic structure of $\text{SrFe}_{12}\text{O}_{19}$ in Gorter's spin structure was calculated and volumetric optimizations were performed to obtain the respective ground states.

B. Hybrid functionals

Hybrid density functionals have much more accuracy than GGA functionals. But they are computationally expensive for large systems. Available Hybrid functionals include a certain amount of the Hartree-Fock exchange. The HSE scheme is a screened Coulomb functional that is based on the GGA (PBE) exchange functional with a short-range modification. The accuracy of the HSE hybrid functional is comparable to B3LYP and PBE0 functionals whereas it considerably reduces the computational effort. It has been successfully applied for large molecules and periodic systems.³³ To determine the U value we calculated the electronic structure of $\text{SrFe}_{12}\text{O}_{19}$ using HSE functionals. HSE calculation was started from the results of the GGA calculation. The volumetric relaxed structure and charge densities of $\text{SrFe}_{12}\text{O}_{19}$ from the GGA calculation were used to obtain the energy and magnetic moments through HSE calculations. The U value which reproduced the average magnetic moments of each symmetry site of the unit cell closest to the HSE calculation was then chosen.

III. RESULTS

A. Pure $\text{SrFe}_{12}\text{O}_{19}$

Pure SrM ($\text{SrFe}_{12-x}(\text{Zn}_{0.5}\text{Sn}_{0.5})_x\text{O}_{19}$ with $x = 0$) has the hexagonal crystal structure and the space group $P6_3/mmc$ as shown in Fig. 1. As shown in Table I, the unit cell has 11 inequivalent sites: one Sr site of multiplicity 2, five Fe sites of multiplicity 2, 2, 4, 4 and 12, and five oxygen sites of multiplicity 4, 4, 6, 12, and 12. In total the double formula unit cell has 64 atomic sites. First, using GGA functional form we optimized the crystal structure of pure SrM using volumetric and ionic optimizations. The optimized structure was then used to determine magnetic properties of pure SrM crystal through a static calculation using HSE hybrid functional. Finally the variation of magnetic properties with respect to effective U parameter of the GGA+U method was determined through fully optimized calculations. The dependence of the total magnetic moment of the unit cell and the atomic magnetic moments of individual symmetry sites for Fe^{+3} ions on the parameter U is plotted in Fig. 2 and Fig. 3. The values from HSE functional and the nominal value

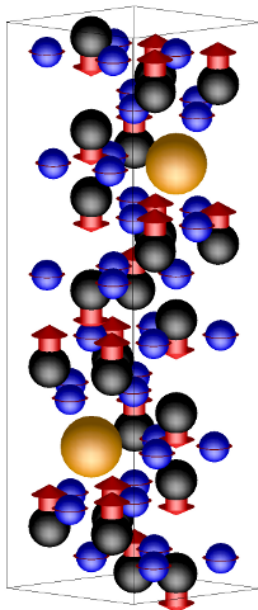


FIG. 1. (Color online) One double formula unit cell of pure $\text{SrFe}_{12}\text{O}_{19}$ in Gorter's spin configuration. Black spheres are Fe atoms, blue spheres are O atoms, and orange spheres are Sr atoms.

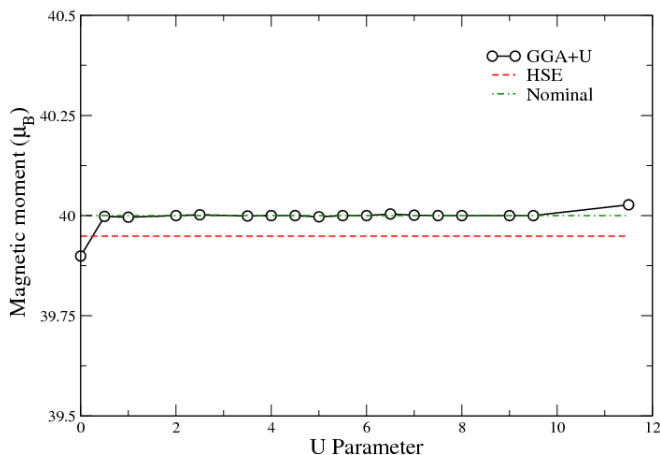


FIG. 2. (Color online) Variation of the total magnetic moment of the unit cell with respect to the effective U parameter for the Gorter's configuration of SrM. The values from calculations using HSE functional and the nominal value are shown as horizontal lines.

($40 \mu_B$) are also shown as horizontal lines for comparison. Fig. 2 shows that the total magnetic moment M_s does not serve as a good criteria for determining the appropriate U value as it is nearly constant over a wide range of U values. On the other hand, Fig. 3 shows that the magnetic moments on inequivalent sites vary smoothly over the range of U values we considered and, more importantly, they cross their corresponding values of HSE calculation *simultaneously* near $U = 3.7$ eV. Therefore, we set U to 3.7 eV for GGA+U method for all subsequent

TABLE I. Average magnetic moments of atoms in $\text{SrFe}_{12}\text{O}_{19}$ calculated using GGA, GGA+U (with $U = 3.7$ eV), and HSE functionals. Total magnetic moment of the double unit cell is also given. All moments are given in μ_B .

site	GGA	GGA+U	HSE
Sr(2d)	-0.005	-0.003	-0.008
Fe(2a)	3.733	4.156	4.149
Fe(2b)	3.541	4.057	4.044
Fe(4f ₁)	-3.426	-4.038	-4.042
Fe(4f ₂)	-3.166	-4.095	-4.093
Fe(12k)	3.719	4.170	4.138
O(4e)	0.383	0.353	0.391
O(4f)	0.121	0.089	0.093
O(6h)	0.085	0.027	0.031
O(12k)	0.093	0.084	0.082
O(12k)	0.175	0.180	0.196
Total	39.89	40.00	39.95

calculations.

Through volumetric and ionic optimizations, we obtained $a = 5.93$ Å and $c = 23.20$ Å as equilibrium lattice constants in good agreement with experimental values of 5.88 Å and 23.04 Å, respectively.³⁸ The total densities of states (DOS) for the optimized Gorter's configuration calculated with HSE, GGA+U ($U = 3.7$ eV) and GGA are shown in Fig. 4. HSE and GGA+U predict an insulating state while GGA predicts a metallic state with nonzero DOS at Fermi energy. The magnetic moments of individual atoms of the 11 inequivalent atomic sites and the saturation magnetic moment of the unit cell, from GGA, GGA+U and HSE functional forms are given in Table I. Individual magnetic moments of the Fe sites predicted by GGA are much less than those by HSE. GGA+U's prediction of the atomic magnetic moments is in good agreement with HSE results. Total magnetic moment values are similar to the nominal value of $40 \mu_B$ per unit cell for all three methods.

B. $\text{SrFe}_{12-x}(\text{Zn}_{0.5}\text{Sn}_{0.5})_x\text{O}_{19}$ with $x = 1$

For $x = 1$ concentration, one Zn and one Sn atom are substituted to two of the 24 Fe sites of unit cell as shown in Fig. 5. All Fe sublattices listed in Table I have more than one equivalent atomic site. In general substitution of Zn-Sn atoms breaks the symmetry among the equivalent sites of pure SrM. Out of all 552 ($= 24 \times 23$) possible Zn-Sn-substituted SrM structures, the 24 symmetry operations of the space group $P6_3/mmc$ render substantial number of structures equivalent leaving only 55 inequivalent structures. We label these inequivalent configurations using the convention of $\text{Zn}(\text{site for Zn})\text{Sn}(\text{site for Sn}).(\text{unique index})$. For example, when Zn and Sn are substituted to 2b and 12k sites, respectively, there are 24 ($= 12 \times 2$) possible structures but only two of them are inequivalent configurations due to symmetry. Therefore, they are labeled as

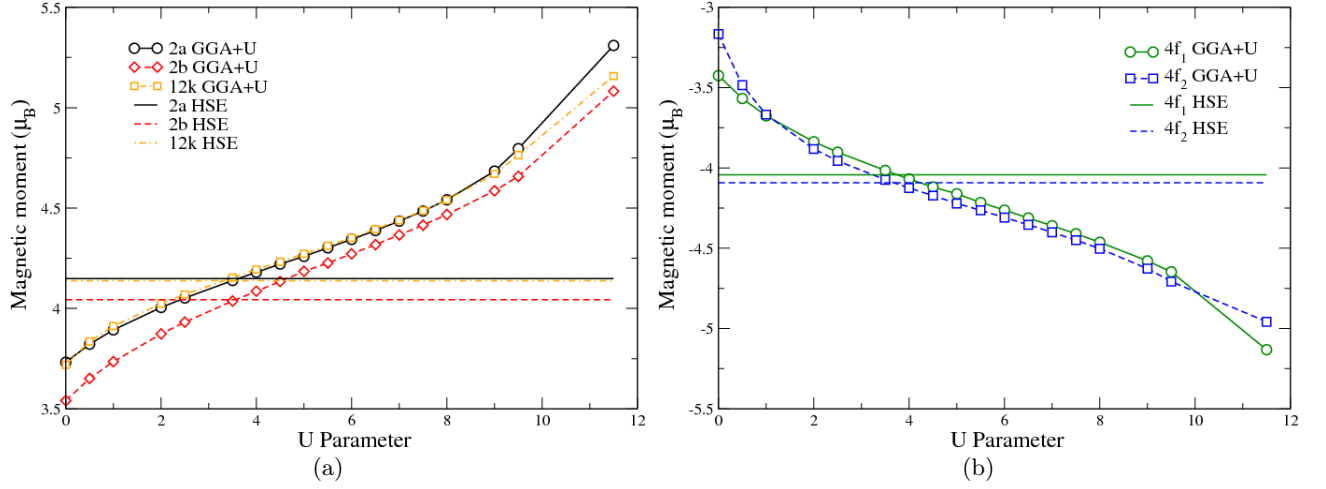


FIG. 3. (Color online) Variation of atomic magnetic moments with respect to the effective U parameter for the Goter's configuration of SrM ; (a) positive magnetic moments for 2a, 2b, and 12k sites and (b) negative magnetic moments for 4f₁ and 4f₂ sites. The values from calculations using HSE functional are shown as horizontal lines.

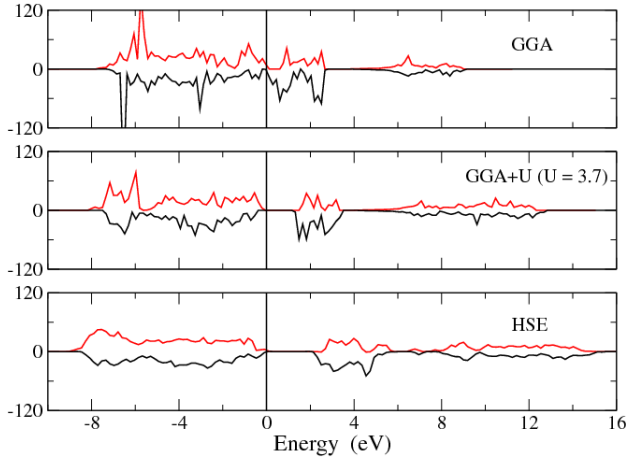


FIG. 4. (Color online) Total densities of states (DOS) (states/eV) of SrFe₁₂O₁₉ calculated using GGA, GGA+U ($U = 3.7$ eV), and HSE methods. Positive values in red correspond to spin-up states and negative values in black correspond to spin-down states. Energy band gaps are measured to be 0.0, 0.93, and 1.19 eV, respectively.

Zn(2b)Sn(12k).1 and Zn(2b)Sn(12k).2. These structures were constructed by substituting Zn and Sn atoms to the respective sites of a SrM unit cell fully optimized using GGA+U ($U = 3.7$ eV). After substitution, the atomic positions of the structures and spin polarized electron charge densities were fully optimized and their total energies were compared. All configurations maintained the original hexagonal structure.

In Table II we lists the ten lowest energy configurations among all inequivalent Zn-Sn-substituted SrM structures we considered. The ground state configuration Zn(4f₁)Sn(4f₂).1 that has Zn and Sn atoms substituted to 4f₁ and 4f₂ sites, respectively, has an increase in M_s of approximately 10 μ_B with respect to pure

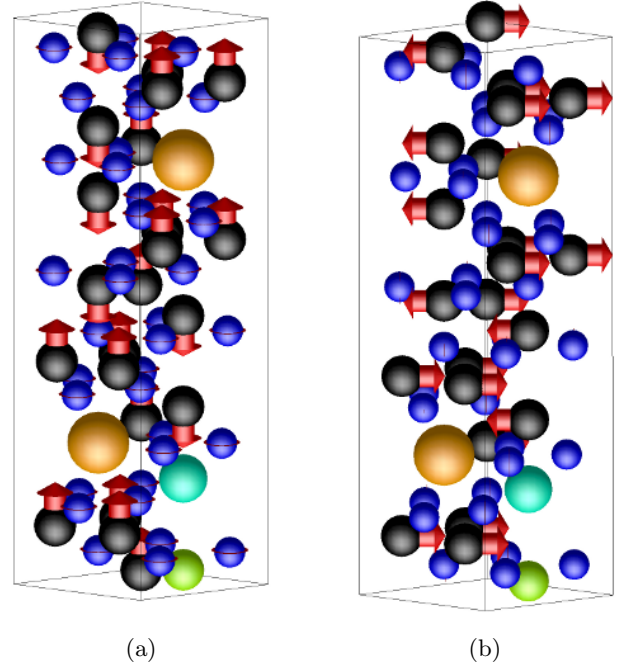


FIG. 5. (Color online) The ground state structure of Zn-Sn-substituted SrM (configuration Zn(4f₁)Sn(4f₂).1) with spins oriented in (a) easy axis (001) and (b) hard axis (100). Black spheres are Fe atoms, blue spheres are O atoms, orange spheres are Sr atoms, green sphere is Zn atom and light blue sphere is Sn atom.

SrM consistent with the experimental results by Ghasemi and co-workers.^{7,20} The structure suggested by Ghasemi with Zn²⁺ in 2b site and Sn⁴⁺ in 4f₂ site (configuration Zn(2b)Sn(4f₂).1 in Table II) is an excited state configuration ranked #8 with a much higher total energy (0.277 eV). Furthermore, configuration Zn(2b)Sn(4f₂).1 shows nearly no increase in M_s contradicting the exper-

TABLE II. Ten lowest energy configurations of Zn-Sn-substituted SrM $\text{SrFe}_{12-x}(\text{Zn}_{0.5}\text{Sn}_{0.5})_x\text{O}_{19}$ for $x = 1$. Total energies (E_{tot}) are relative to that of the ground state configuration $\text{Zn}(4f_1)\text{Sn}(4f_2).1$. Saturation magnetic moment (M_s) and the change in M_s with respect to pure SrM in Gorter's configuration (ΔM_s) are also given. All values are for a double formula unit cell of $\text{SrFe}_{12-x}(\text{Zn}_{0.5}\text{Sn}_{0.5})_x\text{O}_{19}$ containing 64 atoms. All energies are given in eV while magnetic moments are given in μ_B .

index	config	E_{tot}	M_s	ΔM_s
1	$\text{Zn}(4f_1)\text{Sn}(4f_2).1$	0.000	50.002	10.001
2	$\text{Zn}(4f_1)\text{Sn}(4f_2).4$	0.158	50.001	10.000
3	$\text{Zn}(12k)\text{Sn}(4f_2).3$	0.177	40.007	0.006
4	$\text{Zn}(4f_1)\text{Sn}(4f_2).3$	0.187	50.000	9.999
5	$\text{Zn}(4f_1)\text{Sn}(12k).3$	0.190	40.000	-0.001
6	$\text{Zn}(4f_1)\text{Sn}(4f_2).2$	0.257	50.001	10.000
7	$\text{Zn}(4f_1)\text{Sn}(2a).1$	0.265	39.998	-0.002
8	$\text{Zn}(2b)\text{Sn}(4f_2).1$	0.277	40.003	0.002
9	$\text{Zn}(2a)\text{Sn}(4f_2).1$	0.277	40.001	-0.000
10	$\text{Zn}(12k)\text{Zn}(4f_2).2$	0.384	40.000	0.000

imental result showing a rapid increase of M_s with concentration x ($\sim 7\%$ increase at $x = 1$). We note that configurations with Zn and Sn substituted in $4f_1$ and $4f_2$ sites show considerable increase in M_s ($\sim 10 \mu_B$) while those with $2a$, $2b$, and $12k$ sites show nearly zero increase in M_s .

In Table III we compared the contribution of different sublattices to the total magnetic moment in these two proposed models for the structure of Zn-Sn-substituted SrM. To see the effect of Zn and Sn atoms in different sublattices, we split the entries of sublattices containing these atoms ($4f_1$, $4f_2$, and $2b$). As expected, Zn^{2+} and Sn^{4+} ions carry negligible magnetic moments regardless of their substitution sites. Consequently, when they replace Fe^{3+} ions in the minority spin sites ($4f_1$ and $4f_2$), they eliminate negative contribution and make positive contribution. On the other hand, when Zn^{2+} and Sn^{4+} ions replace Fe^{3+} ions in the majority spin site ($2b$), they eliminate positive contribution and make negative contribution. Therefore, configuration $\text{Zn}(4f_1)\text{Sn}(4f_2).1$ results in an increase of $10 \mu_B$ for the saturation magnetic moment M_s , whereas configuration $\text{Zn}(2b)\text{Sn}(4f_2).1$, where Zn and Sn are substituted to $2b$ and $4f_2$ sites, shows no increase in M_s as the effect of Zn in $2b$ site cancels out that of Sn in $4f_2$ site.

In addition to increase of M_s , Ghasemi et al. also reported a rapid decrease in anisotropy of SrM due to Zn and Sn substitution.⁷ The decrease in anisotropy was attributed to the substitution of Zn^{2+} ions to $2b$ site. We calculated magnetic anisotropy energy (MAE) for the two competing models. A self-consistent calculation on the completely relaxed crystal structure was performed

and the charge densities were extracted. Then non-self-consistent calculations were performed to structures with the spin quantization axis oriented in the easy and hard axes. Fig. 5 shows the optimized ground state configuration $\text{Zn}(4f_1)\text{Sn}(4f_2).1$ with magnetic moments in the easy axis and the hard axis. MAE is the difference of total energies from these calculations:

$$E_{\text{MAE}} = E_{(100)} - E_{(001)}$$

where $E_{(100)}$ is the total energy with spin quantization axis in the hard direction (y -axis) and $E_{(001)}$ the total energy with spin quantization axis in the easy direction (x -axis). Using the MAE, magnetic anisotropy constant K can be computed:

$$K = \frac{E_{\text{MAE}}}{V \sin^2 \theta}$$

where V is the equilibrium volume and θ is the angle between the two spin quantization axis orientations (90deg in this case). Results of these calculations are presented in Table IV, which shows that both the configurations show rapid decrease in anisotropy consistent with the experimental results.

IV. CONCLUSION

Using first-principles total energy calculations based on density functional theory, we obtained the ground state structure for Zn-Sn-substituted SrM, $\text{SrFe}_{12-x}(\text{Zn}_{0.5}\text{Sn}_{0.5})_x\text{O}_{19}$ with $x = 1$. We showed that Zn and Sn atoms preferentially occupy $4f_1$ and $4f_2$ sites. The stable structure derived from our calculations shows a rapid increase in saturation magnetic moment and a significant decrease in magnetic anisotropy with respect to pure SrM that is consistent with experimental observations. We showed that the previously proposed model with Zn atom in $2b$ is an excited configuration with significantly higher total energy and consequently unlikely to be formed in thermodynamic limit. We also showed that the decrease in magnetic anisotropy is not associated specifically with $2b$ site.

V. ACKNOWLEDGMENT

This work was supported in part by the U.S. Department of Energy ARPA-E REACT program under Award Number DE-AR0000189, the Center for Advanced Vehicular Systems (CAVS), and the Center for Computational Science (CCS) at Mississippi State University. Computer time allocation has been provided by the High Performance Computing Collaboratory (HPC²) at Mississippi State University.

TABLE III. Contribution of sublattices to the total magnetic moment of Zn-Sn-substituted SrM structures Zn($4f_1$)Sn($4f_2$).1 and Zn($2b$)Sn($4f_2$).1 compared with pure SrM. All moments are given in μ_B .

site	SrM		Zn($4f_1$)Sn($4f_2$).1			Zn($2b$)Sn($4f_2$).1		
	atoms	m	atoms	m	Δm	atoms	m	Δm
2d	2*Sr	-0.006	2*Sr	-0.003	0.003	2*Sr	-0.003	0.003
2a	2*Fe	8.312	2*Fe	8.468	0.156	2*Fe	8.313	0.001
2b	1*Fe	4.057	1*Fe	4.148	0.091	1*Fe	4.060	0.003
	1*Fe	4.057	1*Fe	4.056	-0.001	1* Zn	-0.013	-4.070
4f ₁	3*Fe	-12.114	3*Fe	-12.071	0.043	3*Fe	-12.099	0.015
	1*Fe	-4.038	1* Zn	0.059	4.097	1*Fe	-4.037	0.001
4f ₂	3*Fe	-12.285	3*Fe	-12.191	0.094	3*Fe	-12.348	-0.063
	1*Fe	-4.095	1* Sn	0.049	4.144	1* Sn	0.034	4.129
12k	12*Fe	50.040	12*Fe	50.219	0.179	12*Fe	50.160	0.120
4e	4*O	1.412	4*O	1.251	-0.161	4*O	1.411	-0.001
4f	4*O	0.356	4*O	0.346	-0.010	4*O	0.333	-0.023
6h	6*O	0.164	6*O	0.422	0.258	6*O	-0.087	-0.251
12k	12*O	1.004	12*O	1.034	0.030	12*O	1.016	0.012
12k	12*O	2.156	12*O	3.106	0.950	12*O	2.328	0.172
Total		40.001		49.957	9.956		30.964	-0.037

TABLE IV. Magnetic anisotropy energy (MAE) and magnetic anisotropy constant K for two of the $x = 1$ configurations of Zn-Sn-substituted SrM and pure SrM.

Config	MAE (meV)	K (kJ·m ⁻³)
SrM	0.84	190
Zn($4f_1$)Sn($4f_2$).1	0.45	100
Zn($2b$)Sn(f_2).1	0.56	120

- * Author to whom correspondence should be addressed; kimsq@ccs.msstate.edu
- ¹ Z. Pang, X. Zhang, B. Ding, D. Bao, and B. Han, Journal of Alloys and Compounds **492**, 691 (2010).
 - ² a. Davoodi and B. Hashemi, Journal of Alloys and Compounds **509**, 5893 (2011).
 - ³ M. N. Ashiq, M. J. Iqbal, M. Najam-ul Haq, P. Hernandez Gomez, and A. M. Qureshi, Journal of Magnetism and Magnetic Materials **324**, 15 (2012).
 - ⁴ Q. Fang, H. Cheng, K. Huang, J. Wang, R. Li, and Y. Jiao, Journal of Magnetism and Magnetic Materials **294**, 281 (2005).
 - ⁵ G. Asghar and M. A. ur Rehman, Journal of Alloys and Compounds **526**, 85 (2012).
 - ⁶ M. N. Ashiq, M. Javed Iqbal, and I. Hussain Gul, Journal of Magnetism and Magnetic Materials **323**, 259 (2011).
 - ⁷ A. Ghasemi, V. Šepelák, X. Liu, and A. Morisako, Journal of Applied Physics **107**, 09A734 (2010).
 - ⁸ M. J. Iqbal, M. N. Ashiq, and P. H. Gomez, Journal of Alloys and Compounds **478**, 736 (2009).
 - ⁹ P. Bercoff, C. Herme, and S. Jacobo, Journal of Magnetism and Magnetic Materials **321**, 2245 (2009).
 - ¹⁰ T. Nga, N. Duong, and T. Hien, Journal of Alloys and Compounds **475**, 55 (2009).
 - ¹¹ M. N. Ashiq, M. J. Iqbal, and I. H. Gul, Journal of Alloys and Compounds **487**, 341 (2009).
 - ¹² M. J. Iqbal, M. N. Ashiq, P. Hernandez-Gomez, and J. M. Munoz, Journal of Magnetism and Magnetic Materials **320**, 881 (2008).
 - ¹³ N. Rezlescu, C. Doroftei, E. Rezlescu, and P. Popa, Journal of Alloys and Compounds **451**, 492 (2008).
 - ¹⁴ M. J. Iqbal, M. N. Ashiq, P. Hernandez-Gomez, and J. M. Munoz, Scripta Materialia **57**, 1093 (2007).
 - ¹⁵ M. J. Iqbal and M. N. Ashiq, Scripta Materialia **56**, 145 (2007).
 - ¹⁶ L. Qiao, L. You, J. Zheng, L. Jiang, and J. Sheng, Journal of Magnetism and Magnetic Materials **318**, 74 (2007).
 - ¹⁷ J. Wang, C. Ponton, R. Grössinger, and I. Harris, Journal of Alloys and Compounds **369**, 170 (2004).
 - ¹⁸ Q. Fang, Journal of Applied Physics **95**, 6360 (2004).
 - ¹⁹ Q. Fang, W. Zhong, Z. Jin, and Y. Du, Journal of Applied Physics **85**, 1667 (1999).
 - ²⁰ A. Ghasemi and V. Šepelák, Journal of Magnetism and Magnetic Materials **323**, 1727 (2011).
 - ²¹ C. Fang, F. Kools, R. Metselaar, R. Groot, and Others, Journal of Physics: Condensed Matter **15**, 6229 (2003).
 - ²² P. Novák and J. Ruzs, Phys. Rev. B **71**, 1 (2005).
 - ²³ M. Küpferling, P. Novák, K. Knížek, M. W. Pieper, R. Grössinger, G. Wiesinger, and M. Reissner, Journal of Applied Physics **97**, 10F309 (2005).
 - ²⁴ P. Novk, K. Knek, M. Kpferling, R. Grssinger, and M. W. Pieper, The European Physical Journal B - Condensed Matter and Complex Systems **43**, 509 (2005),

- 10.1140/epjb/e2005-00084-8.
- ²⁵ G. Kresse and J. Furthmüller, Phys. Rev. B **54**, 11169 (1996).
 - ²⁶ G. Kresse and D. Joubert, Phys. Rev. B **59**, 1758 (1999).
 - ²⁷ E. F. Gorter, Proc. IEEE **104B**, 2555 (1957).
 - ²⁸ H. Monkhorst and J. Pack, Phys. Rev. B **13**, 5188 (1976).
 - ²⁹ M. Methfessel and A. T. Paxton, Phys. Rev. B **40**, 3616 (1989).
 - ³⁰ P. E. Blöchl, O. Jepsen, and O. K. Andersen, Phys. Rev. B **49**, 16223 (1994).
 - ³¹ Pter and Pulay, Chemical Physics Letters **73**, 393 (1980).
 - ³² J. P. Perdew, K. Burke, and M. Ernzerhof, Phys. Rev. Lett. **77**, 3865 (1996).
 - ³³ J. Heyd, G. E. Scuseria, and M. Ernzerhof, The Journal of Chemical Physics **118**, 8207 (2003).
 - ³⁴ J. Heyd and G. E. Scuseria, The Journal of Chemical Physics **121**, 1187 (2004).
 - ³⁵ J. Heyd, G. E. Scuseria, and M. Ernzerhof, The Journal of Chemical Physics **124**, 219906 (2006).
 - ³⁶ S. H. Vosko, L. Wilk, and M. Nusair, Canadian Journal of Physics **58**, 1200 (1980), <http://www.nrcresearchpress.com/doi/pdf/10.1139/p80-159>.
 - ³⁷ S. L. Dudarev, G. A. Botton, S. Y. Savrasov, C. J. Humphreys, and A. P. Sutton, Phys. Rev. B **57**, 1505 (1998).
 - ³⁸ K. Kimura, M. Ohgaki, K. Tanaka, H. Morikawa, and F. Marumo, Journal of Solid State Chemistry **87**, 186 (1990).